附件1

浙江工程师学院（浙江大学工程师学院）
同行专家业内评价意见书

姓名： 李龙

学号： 22260385

申报工程师职称专业类别（领域）： 电子信息

浙江工程师学院（浙江大学工程师学院）制

2025年03月25日

1

填表说明

一、本报告中相关的技术或数据如涉及知识产权保护、军工项目保密等内容，请作脱密处理。

二、请用宋体小四字号撰写本报告，可另行附页或增加页数，A4纸双面打印。

三、表中所涉及的签名都必须用蓝、黑色墨水笔，亲笔签名或签字章，不可以打印代替。

四、同行专家业内评价意见书编号由工程师学院填写，编号规则为：年份4位＋申报工程师职称专业类别(领域)4位+流水号3位，共11位。

一、个人申报

（一）基本情况【围绕《浙江工程师学院（浙江大学工程师学院）工程类专业学位研究生工程师职称评审参考指标》，结合该专业类别(领域)工程师职称评审相关标准，举例说明】

1. 对本专业基础理论知识和专业技术知识掌握情况(不少于200字)

在电子信息工程射频方向的专业学习中，我系统掌握了电磁场与微波技术、通信原理、高频电子线路等核心理论课程，具备扎实的专业基础。深入理解麦克斯韦方程组、传输线理论及史密斯圆图的应用，能够熟练运用微波网络分析方法和S参数对射频系统进行建模与分析。在微波器件设计方面，掌握滤波器、功分器、耦合器等无源器件的设计原理，熟悉微带线、同轴结构等实现方式，并能通过ADS、HFSS等EDA工具完成电路仿真与参数优化。

专业技术层面，具备射频收发系统全链路设计能力，涵盖低噪声放大器、混频器、功率放大器等有源电路的设计与调试。熟练掌握阻抗匹配、噪声抑制、线性度优化等关键技术，能结合实际场景进行链路预算计算与系统级指标分解。对天线理论与设计有深入研究，熟悉偶极子、贴片天线及阵列天天的辐射机理，能运用CST进行三维电磁仿真与方向图优化。在测试测量方面，熟练操作矢量网络分析仪、频谱仪等设备，精通S参数测试、互调失真分析等射频特性测试方法，具备较强的实际问题解决能力。

2. 工程实践的经历(不少于200字)

在宁波康复医院仪器与病人管理定位系统建设中，基于RFID技术设计了覆盖全院的定位管理体系。系统通过部署半无源RFID标签与多层级读写器网络实现目标追踪：为医疗设备配置耐高温标签，结合固定读写器完成设备出入库自动记录，利用信号强度优化算法提升定位精度；针对患者管理，采用佩戴式腕带标签实时监测活动区域，通过时序信号分析抑制环境干扰引起的定位偏差。为解决金属环境信号衰减问题，采用定向天线与标签休眠策略优化信号覆盖，后台系统集成电子地图与异常告警功能，最终实现设备高效盘点与患者安全监护的双重管理目标。

3. 在实际工作中综合运用所学知识解决复杂工程问题的案例（不少于1000字）

在参与宁波康复中心智能化管理系统的建设工程中，我负责设计并落地了一套基于射频识别技术的设备与人员定位解决方案。该项目需解决院内医疗设备管理混乱、患者安全监护不足以及复杂电磁环境干扰等系统性难题。通过综合运用电磁场传播理论、通信系统设计、信号处理算法及嵌入式开发技术，最终构建了一套稳定高效的定位管理系统，展现了复杂工程问题中多学科知识的交叉应用能力。

1.
针对于RFID定位系统对于大规模天线阵列的依赖，设计并验证了一种天线加透射超表面的结构。透过超表面对天线发射信号的相位进行控制，以此来达到对远场波束的控制。通过引入PIN二极管调控等效电磁参数，在920 MHz附近展现出优异的相位偏移能力，最大相位偏移达110°，从而实现对入射电磁波相位的精确操控。CST仿真结果表明，正反向传输系数（S21和S12）在工作频段内保持一致，确保了高效能量传输与显著的相位变化。通过测试超表面S参数曲线和近场，验证了超表面的功能并获取了调制的参数，凭借其结构简单、控制灵敏、低成本的特点，有望在RFID定位策略中广泛应用。

2.
针对于RFID定位系统对于目标相对运动的依赖，将关联成像与超表面融合到RFID系统中，并进一步依照系统设计改进关联成像算法，使其在超表面参与的复杂情况下依旧能完成对于标签的准确定位。并通过引入SVD滤除噪声，显著提升了系统的抗噪性能与定位质量。改进后

的算法在不同定位精度下均能实现高精度的目标重建，并成功应对了-80 dBm强度的空间噪声干扰，验证了算法在实际应用中的鲁棒性和优越性。这一研究为雷达关联成像技术在复杂无线环境中的应用提供了理论基础和技术支持，具有重要的应用前景。

3.

基于超表面的设计与算法改进，提出并验证了一整套RFID关联成像定位系统。通过将PC、Impinj R700、天线阵列与超表面有机结合，搭建了一种具有高灵活性和鲁棒性的定位系统，并实现了从理论设计到实际应用的过渡。在数据采集过程中，Java、MATLAB和Labview的协同工作不仅显著提高了系统的实时性，还通过引入文本文件通信机制解决了多模块间数据传输的延迟问题。尤其是在信号处理环节，通过奇异值分解算法对散射信号进行去噪与还原，验证了目标位置的高精度定位效果。系统整体定位功能可以在距离1.5 m处，范围0.8 m 0.8 m的平面上实现0.05 m精度的标签定位。这种集成式设计为未来复杂场景下的RFID定位应用奠定了技术基础。

系统集成与工程实施阶段，面对多子系统数据融合的挑战，设计了轻量级通信协议实现定位数据、设备状态与患者信息的实时同步。通过三维电磁场仿真与现场实测相结合的方式，优化读写器布点方案，确保全院区信号覆盖完整。在调试过程中发现特定医疗设备产生的宽频干扰，通过频谱分析与滤波器参数迭代，最终将误触发率降至可接受范围。整套系统通过模块化设计实现了快速部署，后台管理平台集成电子地图可视化、异常行为预警及数据分析功能，形成完整的闭环管理体系。

（二）取得的业绩（代表作）【限填3项，须提交证明原件（包括发表的论文、出版的著作、专利证书、获奖证书、科技项目立项文件或合同、企业证明等）供核实，并提供复印件一份】

1.
公开成果代表作【论文发表、专利成果、软件著作权、标准规范与行业工法制定、著作编写、科技成果获奖、学位论文等】

成果名称	成果类别 [含论文、授权专利（含发明专利申请）、软件著作权、标准、工法、著作、获奖、学位论文等]	发表时间/授权或申请时间等	刊物名称/专利授权或申请号等	本人排名/总人数	备注
Implementing Tunable Metasurface for an RFID Correlative Imaging Localization System	会议论文	2024年11月08日	IMWS-2024		EI会议收录
一种基于超表面的空间相控阵及控制方法	发明专利申请	2022年12月15日	申请号：202211613627.5	1/5	
基于可调反射面的射频识别关联成像定位系统及方法	发明专利申请	2024年12月26日	申请号：202411934846.2	1/5	

2.其他代表作【主持或参与的课题研究项目、科技成果应用转化推广、企业技术难题解决方案、自主研发设计的产品或样机、技术报告、设计图纸、软课题研究报告、可行性研究报告、规划设计方案、施工或调试报告、工程实验、技术培训教材、推动行业发展中发挥的作用及取得的经济社会效益等】

（三）在校期间课程、专业实践训练及学位论文相关情况	
课程成绩情况	按课程学分核算的平均成绩： 86 分
专业实践训练时间及考核情况(具有三年及以上工作经历的不作要求)	累计时间： 1 年（要求1年及以上） 考核成绩： 77 分

本人承诺

个人声明：本人上述所填资料均为真实有效，如有虚假，愿承担一切责任，特此声明！

申报人签名：李龙

22260385

二、日常表现考核评价及申报材料审核公示结果

日常表现 考核评价	非定向生由德育导师考核评价、定向生由所在工作单位考核评价： ☑优秀　　☐良好　　☐合格　　☐不合格 德育导师/定向生所在工作单位分管领导签字（公章）：　　2025 年 3 月 26 日
申报材料 审核公示	根据评审条件，工程师学院已对申报人员进行材料审核（学位课程成绩、专业实践训练时间及考核、学位论文、代表作等情况），并将符合要求的申报材料在学院网站公示不少于5个工作日，具体公示结果如下： 　　☐通过　　　☐不通过（具体原因：　　　　　　　　　） 工程师学院教学管理办公室审核签字（公章）：　　　　　年　月　日

7

浙 江 大 学 研 究 生 院

攻读硕士学位研究生成绩表

学号：22260385	姓名：李龙		性别：男	学院：工程师学院		专业：电子信息		学制：2.5年	
毕业时最低应获：25.0学分		已获得：27.0学分			入学年月：2022-09		毕业年月：		
学位证书号：			毕业证书号：			授予学位：			

学习时间	课程名称	备注	学分	成绩	课程性质	学习时间	课程名称	备注学分	成绩	课程性质
2022-2023学年秋季学期	创新设计方法		2.0	通过	专业选修课	2022-2023学年春季学期	优化理论基础	2.0	98	专业选修课
2022-2023学年秋季学期	工程技术创新前沿		1.5	80	专业学位课	2022-2023学年春季学期	嵌入式系统设计	2.0	97	专业选修课
2022-2023学年秋季学期	工程伦理		2.0	90	公共学位课	2022-2023学年春季学期	自然辩证法概论	1.0	86	公共学位课
2022-2023学年冬季学期	光电遥感技术与应用		2.0	86	专业选修课	2022-2023学年春季学期	新时代中国特色社会主义理论与实践	2.0	84	公共学位课
2022-2023学年冬季学期	机器视觉及其应用		2.0	82	专业学位课	2022-2023学年春季学期	研究生论文写作指导	1.0	85	专业学位课
2022-2023学年秋冬学期	研究生英语		2.0	91	公共学位课	2022-2023学年春季学期	研究生英语基础技能	1.0	75	公共学位课
2022-2023学年冬季学期	产业技术发展前沿		1.5	88	专业学位课		硕士生读书报告	2.0	通过	
2022-2023学年秋冬学期	高阶工程认知实践		3.0	88	专业学位课					

说明：1.研究生课程按三种方法计分：百分制，两级制（通过、不通过），五级制（优、良、中、

及格、不及格）。

2.备注中"*"表示重修课程。

学院成绩校核章：

成绩校核人：张梦依

打印日期：2025-03-20

会议论文证明：

Implementing Tunable Metasurface for an RFID Correlative Imaging Localization System

Long Li, Bincai Wu, Yulin Zhou, Shilie Zheng, Xiaonan Hui*, Xianmin Zhang
College of Information Science & Electronic Engineering,
Zhejiang University
Hangzhou, China
x.hui@zju.edu.cn

Abstract—This paper proposes a design method for an RFID system that achieves correlative imaging using tunable metasurfaces for tag localization applications. The imaging system is primarily composed of an RFID reader, a transceiver antenna, a host computer, a tunable metasurface, controlling I/O cards, and RFID tags. The RF signal transmitted from the reader to tag and the tag backscattered signal are both modulated by the tunable metasurface. The tag location imaging map is obtained through processing the acquired signals and the generated metasurface arrangement patterns by the correlative imaging algorithm. The designed metasurface unit exhibits high transmittance and a 120-degree phase change within the 920MHz-925MHz frequency band where the RFID operates. By simulating the correlative imaging algorithm for actual scenarios, the position of the tags can be accurately located.

Keywords—RFID, Correlative Imaging, Tunable Metasurface

I. INTRODUCTION

With the rapid advancement of Internet of Things (IoT) technology, everyday life, learning, and work are becoming incredibly convenient. The foundation of IoT realization lies in the collection, transmission, and processing of information. Transmission relies on various heterogeneous networks centered on the Internet [1], information processing is implemented by cloud computing, artificial intelligence, and other information processing units [2], and information collection depends on various types of sensing devices, including RFID [3], sensors, etc. [4]. Consequently, RFID localization systems, as one of them, have also become a hot research topic in recent years. RFID systems can achieve contactless tag transmission and automatic identification through the spatial coupling of wireless radio frequency signals. They can perceive the physical quantities or characteristics of objects in the physical world, such as in logistics and warehousing management, intelligent transportation systems, and intelligent security fields [5]. Developing localization functions on the existing and widely used RFID can rapidly increase the application scenarios.

In recent years, various RFID tag localization methods and systems have been investigated. Using a mobile robot equipped with a wheeled rotary encoder and connected to multiple antennas with a UHF-RFID reader for positioning tag items is proposed [6]. It can locate the tag rather accurately, but it still requires a complex multi-antenna structure. In addition, a radio frequency scanning imaging system for chipless RFID tags that can recognize multi-tag structures with a single antenna is

demonstrated, while it depends on the relative motion of the object [7]. Therefore, how to use a single antenna for tag location imaging without relying on the relative movement of the object, and to establish an appropriate high-precision signal analysis model, is a major challenge that needs to be addressed.

This paper proposes an RFID localization system based on correlative imaging and tunable metasurfaces. Compared with the conventional RFID imaging methods, the complex antenna array is not necessities, besides the correlative imaging is no longer dependent on the movement of the antenna nor tags to locate the tag position.

II. METASURFACE DESIGN AND SIMULATION

The system proposed in this paper achieves the function of correlative imaging tag localization based on existing commercial RFID readers by incorporating a single antenna and a tunable metasurface. The core hardware functionality lies in the phase-modulated transmissive metasurface, hence, the discussion initially focuses on the design and testing of the tunable transmissive metasurface.

A. Tunable Metasurface Structure

As shown in Fig. 1, the designed metasurface array unit should have transmission characteristics for the electromagnetic waves of the reader's operating frequency band, and it can adjust the phase of the transmitting wave by the PIN diode.
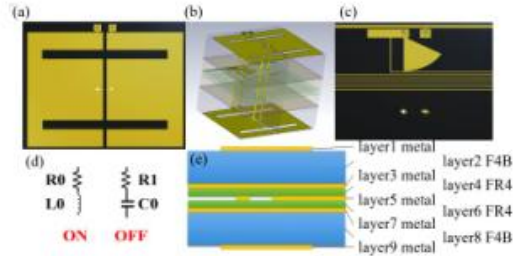

Fig. 1 The tunable metasurface unit structure. (a) The structure of the metasurface unit top (layer1) and bottom (layer9) layer. (b) The 3D explosive view of the metasurface. (c) The pattern of the metasurface interconnection layer (layer5). (d) The equivalent circuits for the PIN diode in the ON and OFF states. (e) The cross section of the metasurface unit.

In order to achieve the above functions, a tunable transmissive surface structure with five layers of metal and two

PIN diodes is designed. The signal given by the PC controls the "on" and "off" of the PIN diodes, making the array unit with two transmissive phase shifts, and 120° phase deflection control of the transmitted signal can be achieved. By continuously feeding the array units random "on" and "off" signals, the transmitted wave with spatial-temporal non-correlation can be achieved. The perspective view and sectional view of the proposed metasurface unit structure are shown in Fig. 1. It comprises a laminated structure with two F4B substrate layers (layer2, layer8 in Fig. 1e) and two FR4 intermediate layers (layer4, layer6) and five metallic layers (layer1, layer3, layer5, layer7 and layer9) bonded together. Two PIN diodes (Skyworks SMP1345-79LF) are embedded in the top and bottom layers of the metasurface to adjust the transmission phase, which is controlled by two bias wires. The equivalent circuits of the PIN diodes in different operating states are shown in Fig. 1(d), where the values of C0, L0, R0, and R1 are 0.165 pF, 0.7 nH, 3 Ω, and 10 Ω, respectively. The direct current (DC) bias wires are deployed on Layer5 and each forward feed wire is connected to an open-circuit stub, which serves as a low-pass filter to isolate the RF and DC signals.

B. Tunable Metasurface Simulation Test

Under the irradiation of TE-polarized incident waves, the metal length along the co-polarized direction of the metasurface unit (shown in Fig. 2(a)) can change the resonant frequency and Q factor of the reflection pattern. Similarly, the size and position of the through-hole determine the passband frequency and loss of the transmissive wave. By optimizing these parameters, the metasurface unit can achieve a low-loss transmissive mode operating within the designed frequency band.
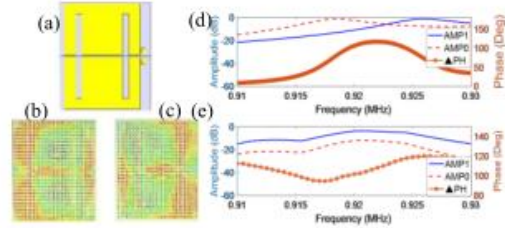

Fig. 2 (a) The metallic pattern on the top and bottom layer of the metasurface unit. (b) The surface current when the diodes are off. (c) The surface current when the diodes are on. (d) The simulated S_{21} amplitude and phase curves of the metasurface. (e) The experimental S_{21} amplitude and phase curves of the metasurface.

The designed metasurface unit can modulate the phase of the transmissive wave by 1 bit. Fig. 2(b) and (c) show the surface current distribution when the diodes are off and on. The cutoff diode is equivalent to the OFF state shown in Fig. 1(d). Since the surface currents in the two states are in different distributions, it indicates that the phase of the transmissive waves will have a significant deflection. As a result, the proposed metasurface unit obtains 1-bit transmission phase modulation. Fig. 2(d) shows the two feeding methods cause a 130° phase change in the S_{21} parameters of the metasurface unit and low insertion loss.

After the metasurface is fabricated, the individual unit of the metasurface is measured with a vector network analyzer using port1 and port2 with external antennas, to measure the phase changes under different conditions. As shown in Fig. 2(e), is the results are in accordance with the simulation results.

III. SYSTEM SIMULATION AND EXPERIMENTAL SETUP

The relationship between the reference signal matrix, received signal matrix, and scattering coefficients of imaging points is no longer linear due to the reference matrix under the metasurface. The signals are the superposition of transmitted signals from each array element after passing through the metasurface. Consequently, the algorithm becomes significantly more computationally challenging. Thus, the received signals are superimposed after processing each pixel individually. Assuming that there is only a target pixel point at (l', k'), r is the position vector of the imaging point, $\boldsymbol{R}$ is the position vector of the metasurface unit, and (p, q) are the row and column indexes of the metasurface. The received signal corresponding to a single pixel point after modulation is represented by Eq. (1).

$$Sr = \sum_{p=0,q=0}^{P,Q} \{a_{loss}S(r_{l'},t_{k'})[n+(1-n)f]D(t_{k'}-\frac{|r_{l'}-\boldsymbol{R}_p|+|r_{k'}-\boldsymbol{R}_q|}{c})\}\sigma_{l'k'}$$
(1)

Where P and Q are the row and column numbers of the metasurface array. n corresponds to the switch state of the PIN diodes. Assuming:

$$S''(r_l,t_k) = \sum_{p=0,q=0}^{P,Q} \{a_{loss}S(r_{l'},t_{k'})[n+(1-n)f]D(t_{k'}-\frac{|r_{l'}-\boldsymbol{R}_p|+|r_{k}-\boldsymbol{R}_q|}{c})\}$$
(2)

Therefore, the aforementioned calculation Eq. (2) can be summarized in the calculation of each imaging point and scattering coefficient as Eq. (3).

$$\begin{bmatrix} Sr(t_1) \\ \vdots \\ Sr(t_K) \end{bmatrix} = \begin{bmatrix} S''(r_1,t_1) & \cdots & S''(r_J,t_K) \\ \vdots & \ddots & \vdots \\ S''(r_J,t_1) & \cdots & S''(r_J,t_K) \end{bmatrix} \cdot \begin{bmatrix} \sigma_1 \\ \vdots \\ \sigma_L \end{bmatrix}$$
(3)

In metasurface imaging, the scattering coefficient is obtained by replacing the calculation with the received signal. It is commonly known as the virtual reference signal for convenience. Therefore, the virtual reference signal can be utilized in place of the original reference signal to achieve tag location imaging.
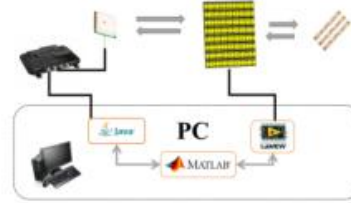

Fig. 3 The schematic of the system.

The system schematic is illustrated in Fig. 3. The computer is connected to an RFID reader (Impinj R700). The tunable

metasurface is controlled by a 48-port I/O card which is connected to the computer. The software is implemented by Java, LabVIEW and MATLAB, in order to drive the RFID reader, control the I/O card and perform the imaging and localization algorithm.

Fig.4 The experimental setup of the system.

With the aforementioned metasurface design, the experimental setup and is built as shown in Fig. 4. The RFID reader is connected to a white patch antenna on the left that transmits and receives the RFID signals. After being modulated by the tunable transmissive metasurface, the signals are received by the tags. The backscattered signal is then modulated by the metasurface again and eventually received by the RFID reader antenna. The metasurface is fed with random "on" and "off" patterns, and the corresponding backscattered signals are recorded for the correlative imaging algorithm.
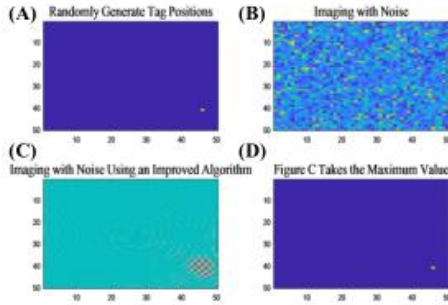

Fig. 5 (a) The ground truth of a tag's location. (b) The original imaging results without algorithm optimization. (c) The improved algorithm imaging result after the optimization. (d) The tag location after the maximum value extraction from (c).

Following the experimental setup, we assume that the noise floor of the reader is −90 dBm, the antenna transmission power is 30 dBm, the distance from the array to the physical object is 2 m, the imaging plane is 2×2 m^2, and the number of random arrangements of the metasurface is 100 patterns. The results are shown in Fig. 5. The tag's signal is overwhelmed by the noise and algorithm artifacts, so the algorithm needs to be optimized. The primary factor contributing to the instability of the least squares solution lies in the fact that a small disturbance in the received echo can lead to a significant alteration in the solution, particularly when associated with a low singular value. Thus, the truncated singular value decomposition method is chosen, where the smaller singular value components in the least squares solution are directly removed. By directly removing the smaller singular value components, the influence of the ambient white noise can be eliminated as much as possible, thereby enhancing the anti-noise ability.

However, as the small singular value components are truncated, the effect of the corresponding eigenvectors is also removed. Therefore, the inversion result obtained does not fully utilize the information about the target scattering coefficient. In addition, since the smaller singular value components often correspond to the high-frequency information in the spatial domain, the action is equivalent to directly performing a windowing operation in the spatial domain, filtering out a negligible amount of useful information and abundant noise interference. As shown in Fig. 5(d), the correct position of the tag can be normally located.

IV. CONCLUSION

The RFID imaging tag localization system proposed in this paper uses a single antenna RFID reader and a tunable metasurface, replacing the complex antenna array, and employs an algorithm for correlative imaging. The system operates within the EPC-RFID frequency band of 920MHz-925MHz.. The metasurface unit is capable of approximately 120° phase deflection and insertion loss of less than 6 dB. The system can achieve the tag localization through the optimized correlative imaging method.

REFERENCES

[1] M. Mansour et al., "Internet of things: A comprehensive overview on protocols, architectures, technologies, simulation tools, and future directions." *Energies,* vol. 16, no. 8, pp. 3465, March 2023.

[2] H. S. Malallah, R. Qashi, L. M. Abdulrahman, M. A. Omer, and A. A. Yazdeen, "Performance analysis of enterprise cloud computing: a review." *Journal of Applied Science and Technology Trends,* vol. 4, no. 01, pp. 01-12, May 2023.

[3] M. M. Mijwil, K. K. Hiran, R. Doshi, and O. J. Unogwu, "Advancing construction with IoT and RFID technology in civil engineering: A technology review." *Al-Salam Journal for Engineering and Technology,* vol. 2, no. 02, pp. 54-62, Mar. 2023.

[4] T. Wang, Y. Liang, X. Shen, X. Zheng, A. Mahmood, and Q. Z. Sheng, "Edge computing and sensor-cloud: Overview, solutions, and directions." *ACM Computing Surveys,* vol. 55, no. 13, pp. 1-37, Jul. 2023.

[5] C. Munoz-Ausecha, J. Ruiz-Rosero, and G. Ramirez-Gonzalez, "RFID applications and security review." *Computation,* vol. 9, no. 6, pp. 69, Jun. 2021.

[6] A. Motroni, F. Bernardini, A. Buffi, P. Nepa, and B. Tellini, "A UHF-RFID multi-antenna sensor fusion enables item and robot localization." *IEEE Journal of Radio Frequency Identification,* vol. 6, pp. 456-466, Apr. 2022.

[7] R. Amorim, N. Barbot, R. Siragusa, and E. Perret, "Chipless RFID tag imaging system based on conveyor-belt radio frequency scanning." *2023 IEEE Conference on Antenna Measurements and Applications (CAMA),* December 2023.

IEEE COPYRIGHT AND CONSENT FORM

To ensure uniformity of treatment among all contributors, other forms may not be substituted for this form, nor may any wording of the form be changed. This form is intended for original material submitted to the IEEE and must accompany any such material in order to be published by the IEEE. Please read the form carefully and keep a copy for your files.

Implementing Tunable Metasurface for an RFID Correlative Imaging Localization System

Long Li, Bincai Wu, Yulin Zhou, Shilie Zheng, Xiaonan Hui, Xianmin Zhang

2024 IEEE MTT-S International Microwave Workshop Series on Advanced Materials and Processes for RF and THz Applications (IMWS-AMP)

COPYRIGHT TRANSFER

The undersigned hereby assigns to The Institute of Electrical and Electronics Engineers, Incorporated (the "IEEE") all rights under copyright that may exist in and to: (a) the Work, including any revised or expanded derivative works submitted to the IEEE by the undersigned based on the Work; and (b) any associated written or multimedia components or other enhancements accompanying the Work.

GENERAL TERMS

1. The undersigned represents that he/she has the power and authority to make and execute this form.
2. The undersigned agrees to indemnify and hold harmless the IEEE from any damage or expense that may arise in the event of a breach of any of the warranties set forth above.
3. The undersigned agrees that publication with IEEE is subject to the policies and procedures of the IEEE PSPB Operations Manual.
4. In the event the above work is not accepted and published by the IEEE or is withdrawn by the author(s) before acceptance by the IEEE, the foregoing copyright transfer shall be null and void. In this case, IEEE will retain a copy of the manuscript for internal administrative/record-keeping purposes.
5. For jointly authored Works, all joint authors should sign, or one of the authors should sign as authorized agent for the others.
6. The author hereby warrants that the Work and Presentation (collectively, the "Materials") are original and that he/she is the author of the Materials. To the extent the Materials incorporate text passages, figures, data or other material from the works of others, the author has obtained any necessary permissions. Where necessary, the author has obtained all third party permissions and consents to grant the license above and has provided copies of such permissions and consents to IEEE

You have indicated that you DO wish to have video/audio recordings made of your conference presentation under terms and conditions set forth in "Consent and Release."

CONSENT AND RELEASE

1. In the event the author makes a presentation based upon the Work at a conference hosted or sponsored in whole or in part by the IEEE, the author, in consideration for his/her participation in the conference, hereby grants the IEEE the unlimited, worldwide, irrevocable

专利一：

国 家 知 识 产 权 局

310013

浙江省杭州市西湖区古墩路 701 号紫金广场 C 座 1506 室 杭州求是
专利事务所有限公司
傅朝栋(057187911326-812) 张法高(0571-87911326)

发文日：

2023 年 04 月 21 日

| 申请号或专利号：202211613627.5 | 发文序号：2023041800875620 |

申请人或专利权人：浙江大学

发明创造名称：一种基于超表面的空间相控阵及控制方法

发 明 专 利 申 请 进 入 实 质 审 查 阶 段 通 知 书

上述专利申请，根据申请人提出的实质审查请求，经审查，符合专利法第 35 条及实施细则第 96 条的规定，该专利申请进入实质审查阶段。

提示：

1.根据专利法实施细则第 51 条第 1 款的规定，发明专利申请人自收到本通知书之日起 3 个月内，可以对发明专利申请主动提出修改。

2.申请文件修改格式要求：

对权利要求修改的应当提交相应的权利要求替换项，涉及权利要求引用关系时，则需要将相应权项一起替换补正。如果申请人需要删除部分权项，申请人应该提交整理后连续编号的部分权利要求书。

对说明书修改的应当提交相应的说明书替换段，不得增加和删除段号，仅只能对有修改部分段进行整段替换。如果要增加内容，则只能增加在某一段中；如果需要删除一个整段内容，应该保留该段号，并在此段后注明："此段删除"字样。段号以国家知识产权局回传的或公布/授权公告的说明书段号为准。

对说明书附图修改的应当以图为单位提交相应的替换附图。

对说明书摘要文字部分修改的应当提交相应的替换页。对摘要附图修改的应当重新指定。

同时，申请人应当在补正书或意见陈述书中标明修改涉及的权项、段号、图、页。

审 查 员：自动审查
联系电话：010-62356655

审查部门：初审及流程管理部

(54) 发明名称
一种基于超表面的空间相控阵及控制方法

(57) 摘要
本发明公开了一种基于超表面的空间相控阵及其控制方法。该空间相控阵包括一个时域反射式超表面阵列和光纤控制单元；时域反射式超表面阵列由超表面单元按阵列形式连续排布而成。光纤控制单元中包含与时域反射式超表面阵列中超表面单元数量相同的光路，所有光路一一对应接入不同超表面单元背部的光电二极管输入端中；每一条光路均能够独立控制输入光电二极管的光强，通过控制各路路的光强来改变时域反射式超表面阵列中不同超表面单元上的光电二极管输出电压以及变容二极管两端的偏置电压，使不同超表面单元产生相应的微波反射谐波分布，从而将光信号直接映射到微波信号上。本发明可实现控制空间电磁波任意方向反射。

专利二
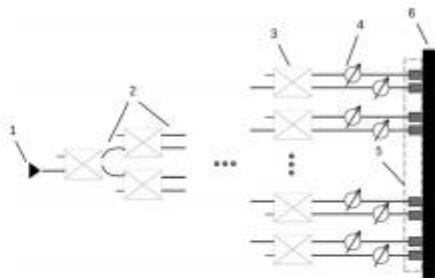
国 家 知 识 产 权 局

310013

浙江省杭州市西湖区古墩路 701 号紫金广场 B 座 1103 室 杭州求是
专利事务所有限公司
傅朝栋(0571-87911726-812)张法高(0571-87911726)

发文日：

2024 年 12 月 26 日

申请号：202411934846.2   发文序号：2024122601046040

专 利 申 请 受 理 通 知 书

根据专利法第 28 条及其实施细则第 43 条、第 44 条的规定，申请人提出的专利申请已由国家知识产权局
受理。现将确定的申请号、申请日等信息通知如下：

申请号：2024119348462
申请日：2024 年 12 月 26 日
申请人：浙江大学
发明人：李龙,回晓楠,吴斌才,李晨铭,章献民
发明创造名称：基于可调反射面的射频识别关联成像定位系统及方法
经核实，国家知识产权局确认收到文件如下：
权利要求书 1 份 3 页,权利要求项数 ： 10 项
说明书 1 份 8 页
说明书附图 1 份 5 页
说明书摘要 1 份 1 页
专利代理委托书 1 份 2 页
发明专利请求书 1 份 5 页
实质审查请求书 文件份数：1 份
申请方案卷号：傅-241-293

提示：

1.申请人收到专利申请受理通知书之后，认为其记载的内容与申请人所提交的相应内容不一致时，可以向国家知识产权局
请求更正。

2.申请人收到专利申请受理通知书之后，再向国家知识产权局办理各种手续时，均应当准确、清晰地写明申请号。

审 查 员：自动受理   审查部门：初审及流程管理部
联系电话：010-62356655